SCIEPublish

Article

Cytosine Deaminase-Assisted Mutator for Genome Evolution in *Cupriavidus necator*

Haojie Pan [1,†], Zhijiao Wang [1,†], Jiazhang Lian [1,2,*]

[1] National Key Laboratory of Biobased Transportation Fuel Technology, College of Chemical and Biological Engineering, Zhejiang University, Hangzhou 310027, China; panhj@zju.edu.cn (H.P.); 22128067@zju.edu.cn (Z.W.)

[2] ZJU-Hangzhou Global Scientific and Technological Innovation Center, Zhejiang University, Hangzhou 311200, China

[†] Haojie Pan and Zhijiao Wang contributed equally to this work.

* Corresponding author. E-mail: jzlian@zju.edu.cn (J.L.)

Received: 13 March 2024; Accepted: 13 June 2024; Available online: 17 June 2024

ABSTRACT: *Cupriavidus necator* H16 has been intensively explored for its potential as a versatile microbial cell factory, especially for its CO_2 fixation capability over the past few decades. However, rational metabolic engineering remains challenging in the construction of microbial cell factories with complex phenotypes due to the limited understanding of its metabolic regulatory network. To overcome this obstacle, laboratory adaptive evolution emerges as an alternative. In the present study, CAM (cytosine deaminase-assisted mutator) was established for the genome evolution of *C. necator*, addressing the issue of low mutation rates. By fusing cytosine deaminase with single-stranded binding proteins, CAM introduced genome-wide C-to-T mutations during DNA replication. This innovative approach could boost mutation rates, thereby expediting laboratory adaptive evolution. The applications of CAM were demonstrated in improving cell factory robustness and substrate utilization, with H_2O_2 resistance and ethylene glycol utilization as illustrative case studies. This genetic tool not only facilitates the development of efficient cell factories but also opens avenues for exploring the intricate phenotype-genotype relationships in *C. necator*.

Keywords: *Cupriavidus necator*; Base editing; ssDNA binding proteins; Genome evolution; Reactive oxygen species; Ethylene glycol

© 2024 by the authors; licensee SCIEPublish, SCISCAN co. Ltd. This article is an open access article distributed under the CC BY license (http://creativecommons.org/licenses/by/4.0/).

1. Introduction

Cupriavidus necator H16, also known as *Ralstonia eutropha* H16, is a versatile facultative chemolithotroph with a notable ability to utilize diverse carbon sources and adapt to various environments [1,2]. It can either grow on fructose and gluconate using the Entner–Doudoroff (ED) pathway or CO_2 through the Calvin-Benson-Bassham (CBB) cycle [3]. *C. necator* has gained great attention in biotechnology for its remarkable performance as a microbial cell factory, especially when integrated into a water-splitting system [4–8]. In this hybrid Microbial Electrosynthesis (MES) system, CO_2 can be converted to high-value products, with the redox equivalent (H_2) originating from electrochemical reactions, providing a promising avenue for achieving carbon neutrality.

Over the last two decades, substantial efforts have been dedicated to transforming *C. necator* into efficient microbial cell factories, yielding a diverse product portfolio encompassing alcohols, fatty acids, and terpenoids [9–11]. While metabolic engineering approaches play an important role and one genome-scale metabolic model [12] is available, the intricacies of the metabolic regulatory network and shortage of genetic engineering tools in *C. necator* pose limitations [11]. Considering this challenge, laboratory adaptive evolution has emerged as a potent alternative strategy to construct chassis strains with complex phenotypes, including enhanced cell factory robustness and substrate utilization [6,13–16]. Especially in conjunction with the rapid advancements of omics tools in recent years, laboratory adaptive evolution proves to be an effective means of exploring the phenotype-genotype relationship. Several studies have successfully employed laboratory adaptive evolution to develop *C. necator* chassis strains with diverse phenotypes, such as improved formate [13] and glycerol [14] utilization, and higher resistance to isobutanol [15] and CO [16].

https://doi.org/10.35534/sbe.2024.10011

Nevertheless, the inherent challenge of a low mutation rate in bacteria presents issues such as prolonged time consumption and low efficiency. Traditional methods such as ultraviolet (UV) [17] and chemical mutagenesis [18] have been adapted to increase the mutation rate in *C. necator*, but they require specialized equipment, chemicals, and sophisticated expertise. To overcome this limitation, genetic mutators capable of disrupting the intracellular mismatch repair mechanism or introducing new mutation mechanisms to increase bacterial mutation rates are promising alternatives [19,20]. Recently, various methods based on the dnaQ mutant library [21,22], cytidine deaminase [23,24], or genome recombination [25] have been established in *Escherichia coli*. For example, cytidine deaminase, such as AID (activation-induced cytidine deaminase) [26] and APOBEC (apolipoprotein B mRNA editing enzyme, catalytic polypeptide-like) [27], can introduce C-T mutations in the genome DNA, thereby increasing mutation rates. However, there is no such method established in *C. necator* to our knowledge, which limits its further application as microbial cell factories.

In this study, CAM (cytosine deaminase-assisted mutator) was established for genome evolution of *C. necator* (Figure 1). To enhance the accessibility of cytosine deaminase to single-stranded DNA, four single-stranded binding proteins involved in the DNA replication process were selected to construct the fusion protein. During DNA replication, the single-stranded binding protein component binds to temporarily exposed single-stranded DNA regions, while the cytosine deaminase component deaminates cytosine (C) to uracil (U), which are then converted to thymine (T) by DNA repair mechanisms. This process introduces C-to-T mutations (or C deletions) in a genome-wide manner, thereby increasing mutation rates and accelerating laboratory adaptive evolution. Using chloramphenicol resistance as an indicator, among the four CAM variants, CAM-dnaB and CAM-SSB exhibited the highest relative mutation rates, representing ~33- and ~11-fold higher than the control strain, respectively. Subsequently, the effect of different CAMs on isopropanol and isobutanol tolerance was evaluated, among which CAM-dnaB and CAM-SSB were still found to perform the best. Finally, the optimal CAM (CAM-dnaB) was chosen for continuous evolution in H_2O_2 resistance and ethylene glycol (EG) utilization, resulting in successful improvement of cell factory robustness and substrate utilization. The present study provides an efficient genome evolution tool to optimize *C. necator* cell factories for diverse biotechnology applications.

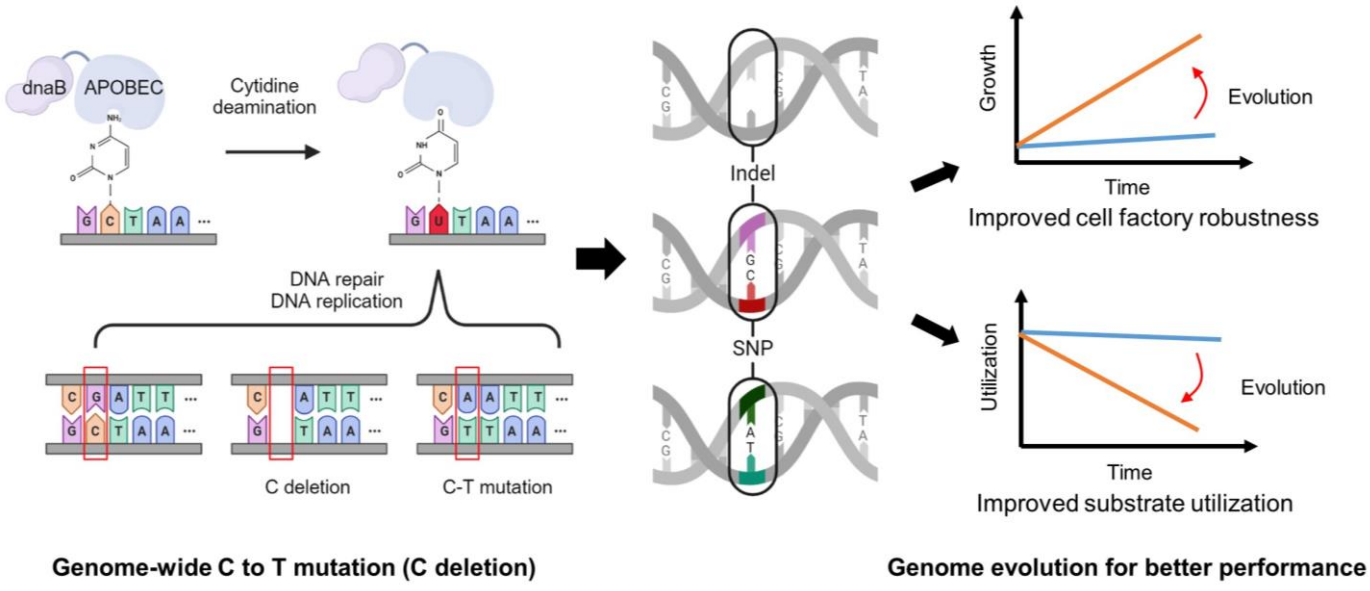

Figure 1. A schematic view of the design of CAM for genome evolution in *C. necator*. By fusing a cytosine deaminase with a single-stranded binding protein, CAM was established to increase mutation rates and expedite laboratory adaptive evolution in *C. necator*. During DNA replication, the single-stranded binding protein component binds to temporarily exposed single-stranded DNA regions, while the cytosine deaminase component deaminates cytosine (C) to uracil (U), which are subsequently deleted or converted to thymine (T) by DNA repair mechanisms. By applying different selective pressures, chassis with desired traits, such as improved cell factory robustness or enhanced substrate utilization, can be obtained in a short time frame.

2. Material and Methods

2.1. Strains and Cultivation Conditions

E. coli was cultured at 37 °C in Luria broth (LB) medium (10 g/L tryptone, 5 g/L yeast extract, and 10 g/L NaCl) with 50 μg/mL kanamycin (Sangon, Shanghai, China) when necessary. *E. coli* DH5α was used as a host for plasmid cloning and propagation, while *E. coli* S17 was used for conjugation when introducing genome editing plasmid pK19mobSacB into *C. necator*. *C. necator* C5 [28], whose electroporation efficiency was improved by knocking out *H16_A0006* and *H16_A0008-9*, was cultured at 30 °C in LB medium or Minimal Salt Medium (MSM, Coolaber, Beijing, China) with 200 μg/mL kanamycin when necessary. All chemicals were purchased from Sigma (Sigma Aldrich, St. Louis, MO, USA), unless specified otherwise. Strains used in this study were listed in Supplementary Table S1.

2.2. Plasmid and Strain Construction

CAM plasmids were derived from pBBR1CMS2 (Addgene #85168). Initially, the P_{ara}-*rfp* cassette was inserted into the backbone through Gibson assembly, resulting in the construction of the control plasmid, pBBR-P_{ara}-*rfp*. Subsequently, *Xho*I and *Bam*HI digestion of the control plasmid facilitated the replacement of the *rfp* gene with the corresponding deaminase gene or the CAM gene using Gibson assembly. *APOBEC*h was cloned from the BE4 plasmid [27], while *PmDCA*cn and *APOBEC*cn with codon optimization were synthesized by Qingke Biotechnology (Nanjing, China). All SSB genes were cloned from the genome of *C. necator* and fused to *APOBEC*cn with the XTEN linker. EG verification plasmids and genome editing plasmids were all constructed via Gibson assembly. Recombinant plasmids were transformed into *C. necator* competent cells through electroporation (Bio-Rad, Hercules, CA, USA), as described by Tee KL et al. [29], except for genome editing plasmids, which were conjugated by *E. coli* S17. Details for genome editing in *C. necator* were described by Wang et al. [30]. Plasmids, primers, and gene-coding sequences used in this study were listed in Supplementary Tables S1–S3, respectively. All plasmid files can be accessed at benchling via https://benchling.com/gaomujun/f_/KPFqkAWa-cam/ (accessed on 14 June 2024). All original plasmids listed in Supplementary Table S1 are available upon request.

2.3. Determination of Genomic Mutation Rates with Various CAMs

Chloramphenicol resistance served as an indicator for determining relative mutation rates. After electroporation, three single colonies were selected and cultured in a 24-well plate for 24–36 h. 60 μL seed culture was inoculated into 3 mL LB with 2 mg/mL arabinose and incubated at 30 °C for 48 h. This process was repeated to accumulate mutations. Then, 1 mL of bacterial solution was centrifuged and resuspended in 100 μL LB broth before plating on LB agar plates containing 10 μg/mL chloramphenicol. In parallel, 1 μL of culture was diluted in 1000 μL LB broth and 100 μL was plated on LB agar plates. 2 mg/mL arabinose was also added to LB agar plates to induce CAM and control gene expression, except for the uninduced controls. Colony-forming units (CFU) were counted and mutation rates were calculated using the formula $Mutation\ rate = \frac{CFU_{+\text{chloramphenicol}}}{CFU_{-\text{chloramphenicol}}}$. Relative mutation rates were normalized to those of the control strain C5/rfp.

2.4. Evaluation of Various CAMs for Increasing Isopropanol and Isobutanol Resistance

Seed cultures of four CAM strains and two control strains, C5/rfp and C5/APOBEC, were prepared as described above for determining relative mutation rates. Following two rounds of induction and mutation accumulation, 60 μL seed culture was inoculated into 3 mL LB or LB containing different concentrations of isopropanol (1%, 2%, and 3%) or isobutanol (1%, 1.5%, and 2%) in 24-well plates. 2 mg/mL arabinose was added to induce CAM and control gene expression. Optical density at 600 nm was measured at 9 h, 24 h, and 48 h after inoculation. Each experiment was repeated at least twice, and the representative results were shown (the trend remained consistent).

2.5. Application of CAMs in the Continuous Genome Evolution for H_2O_2 Resistance and EG Utilization

For H_2O_2 resistance evolution, seed culture was prepared as described above and inoculated into LB medium containing 5 mM H_2O_2 and 2 mg/mL arabinose. Re-inoculation was performed by transferring 60 μL to 3 mL fresh LB medium with H_2O_2 increased by 2.5 mM every 36–48 h until reaching 35 mM. After 12 rounds of evolution, three individual dnaB-evolved clones (named eHP1, eHP2, and eHP3) were isolated and evaluated in LB medium and LB medium containing different concentrations of H_2O_2. For EG utilization evolution, seed culture was inoculated into

MSM medium containing 10 g/L EG as the sole carbon source and subculture (5% inoculation to the same medium) was performed every 72 h. After three generations of evolution, an obvious growth advantage with C5/CAM-danB was seen over the control C5/rfp. Three individual clones (named eEG1, eEG2, and eEG3) were isolated for verification and whole genome sequencing.

2.6. Analysis Methods for OD_{600} and EG

The optical density OD_{600} was measured by a Tecan Infinite 200 PRO Microplate Reader (Tecan Trading AG, Männedorf, Switzerland). For each time point, 200 μL cell culture was sampled for the measurement. The concentration of EG was measured by a Shimadzu High Performance Liquid Chromatograph (HPLC) with an Aminex HPX-87H Ion Exclusion Column (300 × 7.8 mm, 5 μm, temperature 35 °C). For each time point, 100 μL cell culture was taken, diluted 1/10, and filtered through 0.22 μm membranes before HPLC analysis. The mobile phase consisted of 5 mM H_2SO_4 flowing at a rate of 0.6 mL per/min. The detection of compounds was achieved using a UV detector set at a wavelength of 210 nm.

2.7. Whole Genome Sequencing of the Evolved Strain with Increased EG Utilization

Three single colonies of eEG (eEG1, eEG2, and eEG3) were isolated and cultured to mid-log phase for whole genome sequencing. Genomic DNA was extracted with SDS method [31] and prepared for generating sequencing library using NEBNext Ultra™ DNA Library Prep Kit for Illumina (NEB, Ipswich, MA, USA). Next-generation sequencing (NGS) was performed by Novogene (Beijing, China) with Illumina NovaSeq PE150. BWA software (V0.7.8) [32] was used for mapping the reads to the reference genome [2] and SAMtools [33] was used for analyzing single-nucleotide polymorphism (SNPs) and Indels. ANNOVAR [34] was used for functional annotation of variants. The raw NGS data have been deposited into NCBI with an accession number of PRJNA1086218. All SNPs and Indels are listed in Supplementary File S2.

3. Results

3.1. Design and Construction of CAM

Cytosine deaminase functions on both RNA and single-stranded DNA, catalyzing the conversion of base C to U. The base U on single-stranded DNA will be base-paired with A during subsequent cell replication and repair processes, resulting in C-T base replacement (or deletion) [26,27,35]. First, the cytotoxicity of APOBECh (codon-optimized for human) and APOBECcn (codon-optimized for *C. necator*) derived from rats [27], as well as PmCDAcn (AID ortholog, codon-optimized for *C. necator*) derived from lamprey [26] were compared. PmCDAcn exhibited high cytotoxicity to *C. necator*, making it nearly impossible to obtain any transformants probably due to leaky expression (Figure 2a). Any observed individual clones likely resulted from "plasmid escape" as there was no discernible growth inhibition effect in liquid culture (Supplementary Figure S1). In contrast, APOBECcn yielded a considerable number of transformants with minimal impact on growth during liquid culture (Figure 2a and Supplementary Figure S1). This result was consistent with prior reports indicating that the cytotoxicity of PmCDA in bacteria was significantly higher than that of APOBEC [20,36]. Based on our previous findings with the Cas9 protein [30], codon optimization was found to be crucial in *C. necator*, and the lower impact of APOBECh on colony-forming units was assumed to result from its low expression level. Consequently, APOBECcn was chosen for the subsequent CAM construction.

Given that APOBEC acts on single-stranded DNA, four single-stranded binding proteins involved in DNA replication process, including DNA helicase dnaB, DNA primase dnaG, and two single-stranded binding proteins of unknown function, SSB and A0402 (Figure 2b), were selected for guiding APOBEC to single-stranded DNAs. Four versions of CAM, constructed by fusing *APOBEC*cn with single-stranded binding proteins encoding genes, were electroporated into *C. necator* along with two control plasmids, pBBR-P_{ara}-*rfp* and pBBR-P_{ara}-*APOBEC*cn. The growth curves of these six bacteria strains were then measured under the induction of 2 mg/mL arabinose. Except for CAM-A0402, other CAMs showed no significant growth inhibitory effects (Supplementary Figure S2). Subsequent measurements of relative mutation rates, using chloramphenicol resistance as an indicator, revealed that C5/CAM-dnaB strain exhibited the highest relative mutation rates, which was 33 times higher than the control strain C5/rfp. C5/CAM-SSB strain showed the second-highest mutation rates, displaying an 11-fold improvement over the control strain (Figure 2c). The results from the un-induced control showed the great tunability of CAM tool, highlighting its potential for diverse applications. (Supplementary Figure S3). Noteworthy, chloramphenicol resistance is a gain-of-function

phenotype, leading to a relatively modest overall increase in the mutation rates with a notable error range. Nevertheless, it effectively represents the desired phenotypes for evolution, which are typically gain-of-function as well.

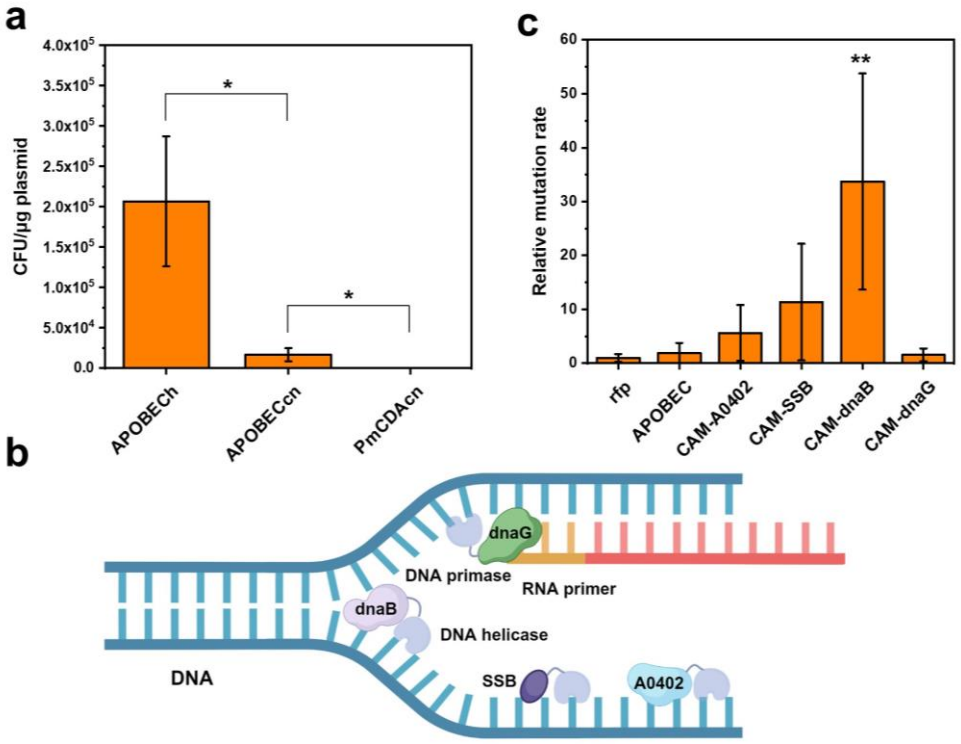

Figure 2. Construction of CAMs with different genomic mutation rates. (**a**) Electroporation efficiency of different cytosine deaminases. Error bars represented the mean ± s.d. of biological triplicates (n = 3). Statistical analysis was performed using a two-sided Student's t test. Selected comparisons were shown. * $p < 0.05$. (**b**) DNA replication related ssDNA binding proteins, including DNA helicase (dnaB), DNA primase (dnaG), and another two proteins with unknown function (SSB and A0402), were chosen for the establishment of CAMs. (**c**) Relative mutation rates of various CAMs with chloramphenicol resistance as an indicator. The mutation rate was normalized to that of the control strain (C5/rfp, set to 1). Error bars represented the mean ± s.d. of 6 biological replicates (n = 6). Statistical analysis was performed using a two-sided Student's t test, with p-value versus the control C5/rfp. ** $p < 0.01$.

3.2. Evaluation of Various CAMs for Increasing Isopropanol and Isobutanol Resistance

After successful construction of CAMs and determination of their mutation rates, a proof-of-concept test was conducted to evaluate their tolerance to isopropanol and isobutanol. The application of *C. necator* for biofuel production, particularly isopropanol and isobutanol, is a prominent area of research [6,37,38], and tolerance to these alcohols is a critical factor limiting their high-yield production. Previous studies explored strategies such as expressing the chaperone protein GroESL to enhance tolerance against isopropanol [39]. However, laboratory adaptive evolution offers a more convenient approach, holding the promise of obtaining strains with superior tolerance. Various CAM strains and two control strains, C5/rfp, and C5/APOBEC, underwent two rounds of induction and mutation accumulation, and then were assessed for their tolerance to different concentration of isopropanol (1%, 2%, and 3%) and isobutanol (1%, 1.5%, and 2%) (Figure 3). As shown in Figure 3a, under 1% isopropanol, CAM strains did not exhibit significant growth advantages, except for CAM-A0402 with heightened cytotoxicity. However, under harsher condition, the growth advantage of CAM became obvious. With 2 % isopropanol, C5/CAM-SSB strain showed a significant growth advantage over other strains after 24 h (Figure 3b). Under the condition of 3% isopropanol, only C5/CAM-dnaB and C5/CAM-SSB strains exhibited robust growth after 48 h, while the other CAM strains and control strains showed no obvious growth. (Figure 3c). These two strains also showed growth advantages over others with isobutanol, which is more toxic than isopropanol (Figure 3d–f). These observed results aligned positively with relative mutation rates (determined through chloramphenicol resistance), suggesting a potential correlation between mutation rates and these resistance phenotypes.

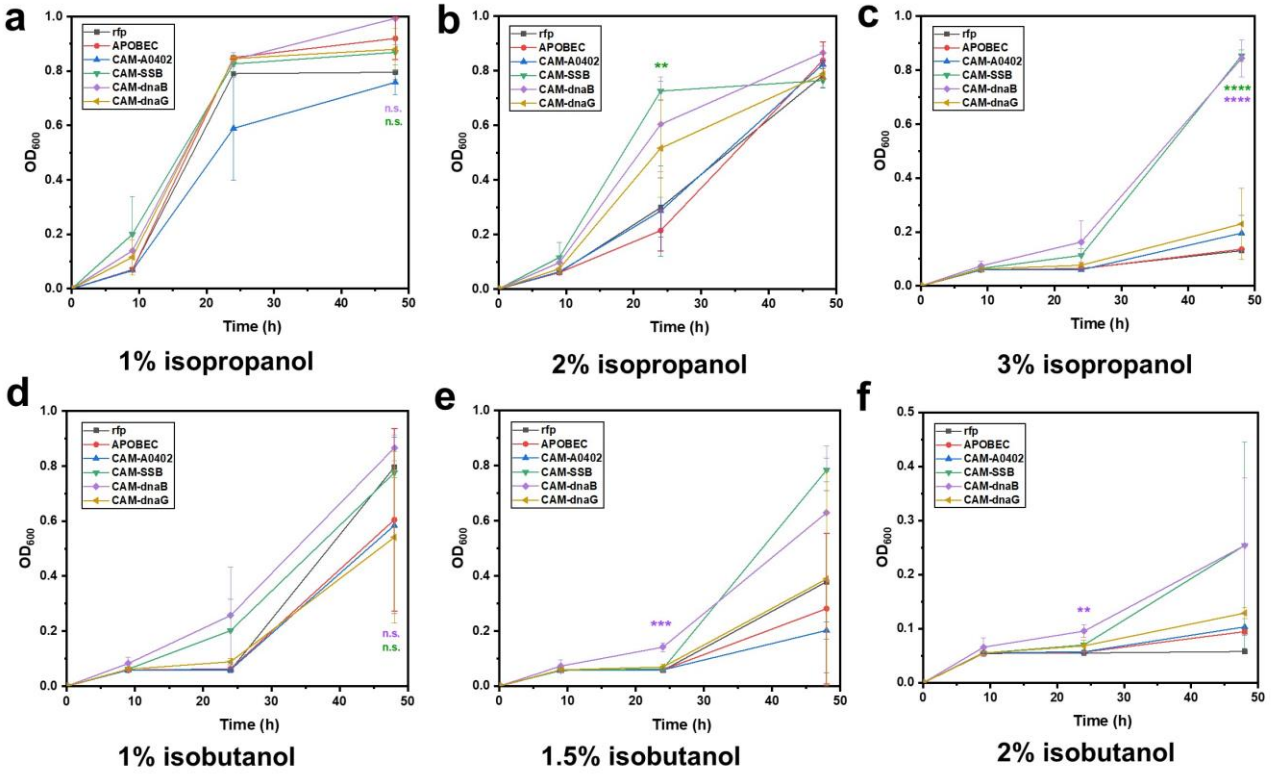

Figure 3. Evaluation of various CAMs for improving isopropanol and isobutanol resistance. Growth curves of CAM strains in LB medium containing isopropanol with a concentration of 1% (**a**), 2% (**b**), and 3% (**c**), and isobutanol with a concentration of 1% (**d**), 1.5% (**e**), and 2% (**f**), respectively. C5/rfp and C5/APOBEC were included as negative controls. Error bars represented the mean ± s.d. of biological triplicates ($n = 3$). Statistical analysis was performed using a two-sided Student's *t* test, with *p*-value versus the control C5/rfp. Statistical designations with different colors referred to the corresponding data points with the same color. n.s. not significant, ** $p < 0.01$, *** $p < 0.001$, **** $p < 0.0001$.

3.3. Application of CAMs in the Continuous Genome Evolution for H_2O_2 Resistance

Following the proof-of-concept test, this genetic tool was validated through improving the compatibility between *C. necator* and inorganic systems within MES system. Given that the toxicity of reactive oxygen species (ROS), particularly H_2O_2, inevitably generated during water electrolysis process is a primary concern [4,6,7], continuous evolution of *C. necator* for high H_2O_2 resistance was performed. Firstly, the tolerance of different CAM strains and control strains to different concentration of H_2O_2 was evaluated. C5/CAM-dnaB and C5/CAM-SSB strains still exhibited superior performance over others (Supplementary Figure S4). Consequently, the most effective C5/CAM-dnaB strain was selected for continuous evolution. Starting from 5 mM H_2O_2, C5/CAM-dnaB strain together with two control strain C5/rfp and C5/APOBEC was exposed to H_2O_2 of incrementally increased concentration in successive passages every 36–48 h. While C5/rfp and C5/APOBEC strains failed to grow at 10 mM H_2O_2, the C5/CAM-dnaB strain showed robust growth at 35 mM H_2O_2 after undergoing 12 rounds of genome evolution (Figure 4a). Three single colonies (named eHP1, eHP2, and eHP3) from the evolved population were selected, and tested under different H_2O_2 concentrations. The robust growth of these colonies at up to 35 mM H_2O_2 indicated stable inheritance of ROS-resistance (Figure 4b,c and Supplementary Figure S5). This strain holds the promise of being a suitable chassis for MES system, potentially offering greater compatibility with the electrolysis process. Establishing a robust, electricity-driven microbial cell factory with improved growth performance will increase the likelihood of achieving real industrial applications for CO_2 valorization in the near future.

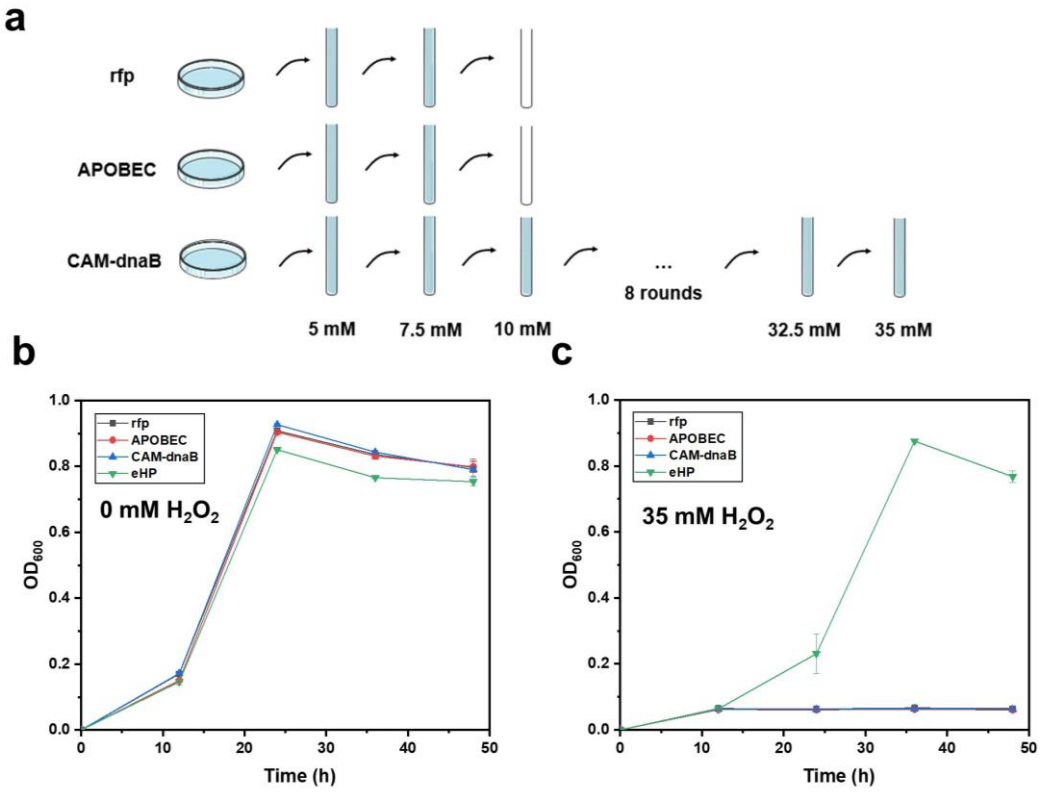

Figure 4. DnaB-mediated continuous evolution of H_2O_2 tolerance. (**a**) Schematic diagram of continuous evolution with CAM-dnaB. After 12 rounds of evolution, three individual dnaB-evolved clones (eHP1, eHP2, and eHP3) were isolated and evaluated in LB medium (**b**) and LB medium containing 35 mM H_2O_2 (**c**), with C5/rfp, C5/APOBEC, and un-evolved C5/CAM-dnaB included as negative controls. Error bars represented the mean ± s.d. of biological triplicates (n = 3).

3.4. Continuous Evolution and Mechanism Elucidation of EG Utilization

EG, a low-cost compound, is considered as a promising next generation feedstock for biomanufacturing, which can be derived from CO_2, syngas, and plastic wastes [40]. As quinate dehydrogenase (QuiA), aldehyde dehydrogenase (ExaC), and pyrroloquinoline quinone (PQQ) are present as the homologs of PedE, PedH, and PQQ in *P. putida* KT2440 [41,42], respectively, *C. necator* is expected to grow on EG. However, the growth rate of the wild-type strain on EG was extremely slow (Figure 5a). Thus, continuous evolution of EG utilization was conducted and an evolved culture eEG was obtained in a short time frame, which outperformed the wild-type strain in growth rate. Three individual clones (named eEG1, eEG2, and eEG3, genome information PRJNA1086218) were isolated for growth and EG consumption evaluation in Minimal Salt Medium (MSM) with EG as the sole carbon source. They exhibited 350 ± 13% higher OD_{600} than the wild-type strain and consumed 7.21 ± 0.90 g/L EG within 48 h (Figure 5a,b).

To elucidate the phenotype-genotype relationship, next-generation sequencing of eEG1, eEG2, and eEG3 was conducted. Several SNPs and indels were identified, and four potential mutations likely associated with enhanced EG metabolism in *C. necator* were found (Table 1). To determine the effective mutations, the above four wild type genes (*pqqD*, *hoxA*, *A0861*, and *B1607*) and their mutants (*pqqD**, *hoxA**, *A0861**, and *B1607**) were overexpressed under the lac promoter (P_{lacRBS}). However, nearly no change in growth profiles was observed in MSM supplemented with EG (Figure 5c and Supplementary Figure S6a). Then, a series of knock-out strains were constructed, whereas most engineered strains retained the original phenotype except for eEGΔ*A0861* (Figure 5d and Supplementary Figure S6b). Interestingly, overexpression of *A0861** failed to improve EG utilization in the wild-type strain, while the evolved strain eEG lost its capacity for rapid growth on EG upon deletion of *A0861**, which should theoretically be deactivated by the frameshift mutation (Figure 5e). Therefore, the flanking sequences of *A0861* on the genome were analyzed before and after mutation. It was observed that an additional start codon (ATG) appeared upstream of the original one (GTG), resulting in the expression of a new potential open reading frame (named *A0861*w, which was 73 bp longer than *A0861*). The frameshift mutation (G deletion) serendipitously caused eEG to express the new protein A0861w* consisting of 391 amino acids rather than A0861 (Figure 5e). Subsequently, *A0861*w and *A0861*w* were overexpressed in the wild type, only *A0861*w* restored the phenotype of eEG. Notably, the original promoter (P_{A0861}) outperformed P_{lacRBS}, likely

due to different expression levels (Figure 5f). These results demonstrated that A0861w* exhibited high alcohol dehydrogenase activity in *C. necator* H16, thereby accelerating EG utilization. Through Protein-BLAST analysis, A0861w* [2] shared high similarity with iron-containing alcohol dehydrogenase in other *C. necator* species, such as *C. necator* C39 (99.74% alignment) and *C. necator* CR12 (99.74% alignment), as well as *E. coli* (75% alignment) (Supplementary Figure S7). It was hypothesized that ancestral strains of *C. necator* H16 had the highly active protein A0861w*, which was inactivated during natural evolution, potentially harboring unknown additional capabilities or adaptations that merit further exploration.

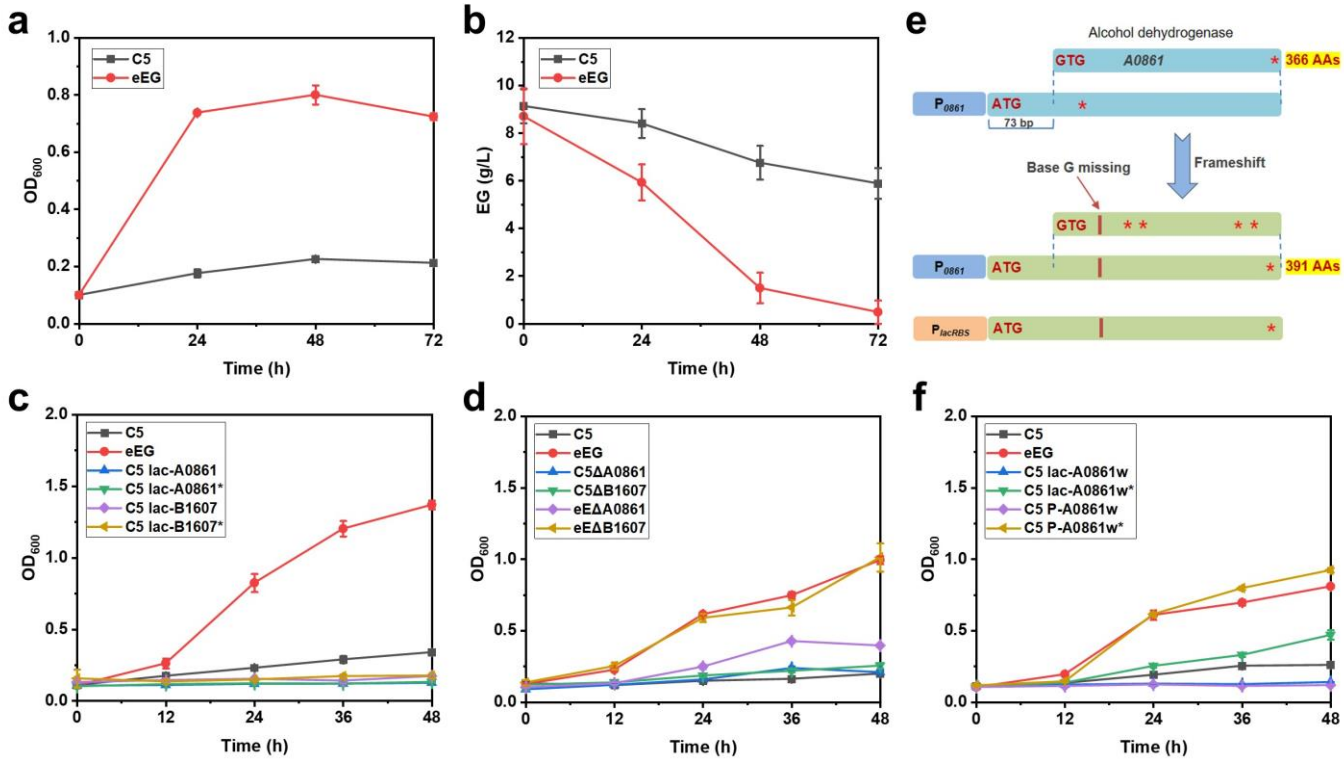

Figure 5. Continuous evolution and mechanism elucidation of EG utilization. (**a**) Growth curves of the evolved strain eEG and the control strain C5 in MSM with EG as the sole carbon source. (**b**) EG utilization by the evolved strain eEG and the control strain C5. (**c**) Mutation analysis by gene overexpression. (**d**) Mutation analysis by gene deletion. (**e**) Gene analysis with base G missing within *A0861*. Red * represent mutations within the protein. (**f**) Strain with increased EG utilization reconstructed by overexpressing full length A0861w*. Error bars represented the mean ± s.d. of biological triplicates (n = 3).

Table 1. Summary of interesting mutations from the evolved strain eEG.

	Chromosome	Position	Mutation	Gene/Protein
eEG	NZ_CP039287.1	947565	Deletion: G	*h16_A0861*/iron-containing alcohol dehydrogenase
	NZ_CP039288.1	1186143	T→C	*pqqD*/pyrroloquinoline quinone biosynthesis peptide chaperone
	NZ_CP039288.1	1813805	Insertion: IS*	*h16_B1067*/AAA- ATPase
	NZ_CP039289.1	16651	G→A	*hoxA*/Sigma-54-dependent Fis family transcriptional regulator

*: The transposable element/1321bp Insertion Sequence.

4. Discussion and Conclusions

Laboratory adaptive evolution is a powerful genetic tool for synthetic biology applications. In the present study, the CAM tool was established for genome evolution in *C. necator*, employing the fusion of cytosine deaminase with a single-stranded binding protein to induce genome-wide C-to-T mutations during DNA replication. The CAM variants, particularly CAM-dnaB, exhibited significantly increased mutation rates and evolutionary advantages towards alcohol- and H_2O_2-resistance. Then CAM-dnaB was applied for continuous evolution in H_2O_2 resistance and EG utilization, resulting in substantial improvements in cell factory robustness and substrate utilization. Furthermore, whole genome

sequencing and reversed metabolic engineering revealed that the alcohol dehydrogenase A0861w* was key to the enhanced EG utilization.

Compared to traditional method like UV and chemical mutagenesis, CAM stands out for its safety, controllability, and ease of use. Its user-friendly nature makes it accessible to a wider range of researchers, eliminating the need for specialized equipment and expertise. While the CAM tool demonstrated notable advantages in the mentioned evolution, there is room for improvement to meet diverse application requirements. In laboratory adaptive evolution, the efficacy of the diversity library significantly impacts the overall efficiency. Enhancing the mutation rate can be achieved by fusing CAM with uracil DNA glycosylase inhibitor (UGI), preventing base corrections [27]. Additionally, substituting CBE with ABE allows for inducing genome-wide A-to-G mutations during DNA replication, broadening the spectrum of mutation types [43]. Furthermore, combining different methods of introducing mutations, such as integrating CAM with CRISPRi-mutator [30], offers a comprehensive approach to introducing genetic diversity.

Laboratory adaptive evolution emerges as a potent tool for engineering complex phenotypes in *C. necator*, addressing challenges posed by the limited understanding of its metabolic and regulatory network. In this study, a strain exhibiting improved utilization of EG was successfully obtained, which holds potential as a chassis for poly(ethylene terephthalate) (PET) valorization. Additionally, the H_2O_2-resistant strain can be applied in MES system for CO_2 valorization. Exploring laboratory adaptive evolution with CAM directly in MES is also a promising avenue, considering the diverse growth pressures present in MES system. Combined with rational design, laboratory adaptive evolution is poised to play an increasingly crucial role in shaping the future of *C. necator* cell factories.

In summary, a genome evolution tool CAM was successfully established in *C. necator*, yielding substantial improvements in cell factory robustness and substrate utilization. Further advancements in synthetic biology tools are essential to harness the full potential of *C. necator* as an efficient and resilient microbial cell factory, particularly leveraging its CO_2 fixation capabilities.

Supplementary Materials

The following supporting information can be found at: https://www.sciepublish.com/article/pii/215, Figure S1: Growth curves of *C. necator* bearing different cytosine deaminases; Figure S2: Growth curves of various CAM strains and control strains under non-stressed condition; Figure S3: Inducibility of CAM system; Figure S4: Evaluation of various CAMs for improving H_2O_2 resistance; Figure S5: DnaB-mediated continuous evolution of H_2O_2 tolerance; Figure S6: Mutation analysis of the evolved strain eEG; Figure S7: Protein-BLAST analysis of A0861w*; Table S1: Strains and plasmids used in this study; Table S2: Primers used in this study; Table S3: Genes used in this study; Table S4: Colony-forming units (CFU). Supplementary File S2: all SNPs and Indels of EG evolved strain EG1, EG2 and EG3.

Acknowledgments

We thank Professor Changhao Bi and Professor Xueli Zhang from Tianjin Institute of Industrial Biotechnology, Chinese Academy of Sciences for providing *C. necator* C5.

Author Contributions

Conceptualization, H.P., Z.W. and J.L.; Methodology, H.P. and Z.W.; Validation, H.P. and Z.W.; Formal Analysis, H.P. and Z.W.; Investigation, H.P.; Resources, H.P. and Z.W.; Data Curation, H.P. and Z.W.; Writing–Original Draft Preparation, H.P. and Z.W.; Writing–Review & Editing, H.P., Z.W. and J.L.; Visualization, H.P. and Z.W.; Supervision, J.L.; Funding Acquisition, J.L.

Ethics Statement

Not applicable.

Informed Consent Statement

Not applicable.

Funding

This work was supported by the "Pioneer" and "Leading Goose" R&D Program of Zhejiang (2024C03111), the Natural Science Foundation of China (22278361, 32200052, and 32300053), the Fundamental Research Funds for the Zhejiang Provincial Universities (226-2023-00015), and the Fundamental Research Funds for the Central Universities (226-2022-00214 and 226-2023-00085).

Declaration of Competing Interest

The authors declare that they have no known competing financial interests or personal relationships that could have appeared to influence the work reported in this paper.

References

1. Schlegel HG, Gottschalk G, Von Bartha R. Formation and utilization of poly-β-hydroxybutyric acid by *Knallgas* bacteria (*Hydrogenomonas*). *Nature* **1961**, *191*, 463–465.
2. Pohlmann A, Fricke WF, Reinecke F, Kusian B, Liesegang H, Cramm R, et al. Genome sequence of the bioplastic-producing "Knallgas" bacterium *Ralstonia eutropha* H16. *Nat. Biotechnol.* **2006**, *24*, 1257–1262.
3. Volodina E, Raberg M, Steinbuchel A. Engineering the heterotrophic carbon sources utilization range of *Ralstonia eutropha* H16 for applications in biotechnology. *Crit. Rev. Biotechnol.* **2016**, *36*, 978–991.
4. Wu H, Pan H, Li Z, Liu T, Liu F, Xiu S, et al. Efficient production of lycopene from CO_2 via microbial electrosynthesis. *Chem. Eng. J.* **2022**, *430*, 132943.
5. Krieg T, Sydow A, Faust S, Huth I, Holtmann D. CO_2 to terpenes: Autotrophic and electroautotrophic alpha-humulene production with *Cupriavidus necator*. *Angew. Chem. Int. Ed. Engl.* **2018**, *57*, 1879–1882.
6. Liu C, Colón BC, Ziesack M, Silver PA, Nocera DG. Water splitting-biosynthetic system with CO_2 reduction efficiencies exceeding photosynthesis. *Science* **2016**, *352*, 1210–1213.
7. Li H, Opgenorth PH, Wernick DG, Rogers S, Wu TY, Higashide W, et al. Integrated electromicrobial conversion of CO_2 to higher alcohols. *Science* **2012**, *335*, 1596.
8. Chen X, Cao Y, Li F, Tian Y, Song H. Enzyme-assisted microbial electrosynthesis of poly(3-hydroxybutyrate) via CO_2 bioreduction by engineered *Ralstonia eutropha*. *ACS Catal.* **2018**, *8*, 4429–4437.
9. Panich J, Fong B, Singer SW. Metabolic engineering of *Cupriavidus necator* H16 for sustainable biofuels from CO_2. *Trends Biotechnol.* **2021**, *39*, 412–424.
10. Raberg M, Volodina E, Lin K, Steinbuchel A. *Ralstonia eutropha* H16 in progress: Applications beside PHAs and establishment as production platform by advanced genetic tools. *Crit. Rev. Biotechnol.* **2018**, *38*, 494–510.
11. Pan H, Wang J, Wu H, Li Z, Lian J. Synthetic biology toolkit for engineering *Cupriviadus necator* H16 as a platform for CO_2 valorization. *Biotechnol. Biofuels* **2021**, *14*, 212.
12. Pearcy N, Garavaglia M, Millat T, Gilbert JP, Song Y, Hartman H, et al. A genome-scale metabolic model of *Cupriavidus necator* H16 integrated with TraDIS and transcriptomic data reveals metabolic insights for biotechnological applications. *PLoS Comput. Biol.* **2022**, *18*, e1010106.
13. Calvey CH, Sànchez INV, White AM, Kneucker CM, Woodworth SP, Alt HM, et al. Improving growth of *Cupriavidus necator* H16 on formate using adaptive laboratory evolution-informed engineering. *Metab. Eng.* **2023**, *75*, 78–90.
14. Gonzalez-Villanueva M, Galaiya H, Staniland P, Staniland J, Savill I, Wong TS, et al. Adaptive laboratory evolution of *Cupriavidus necator* H16 for carbon co-utilization with glycerol. *Int. J. Mol. Sci.* **2019**, *20*, 5735.
15. Bernardi AC, Gai CS, Lu J, Sinskey AJ, Brigham CJ. Experimental evolution and gene knockout studies reveal AcrA-mediated isobutanol tolerance in *Ralstonia eutropha*. *J. Biosci. Bioeng.* **2016**, *122*, 64–69.
16. Wickham-Smith C, Malys N, Winzer K. Improving carbon monoxide tolerance of *Cupriavidus necator* H16 through adaptive laboratory evolution. *Front. Bioeng. Biotechnol.* **2023**, *11*, 1178536.
17. Schlegel H. Verwertung von Glucose durch eine Mutante von *Hydrogenomonas* H16. *Biochem. Z.* **1965**, *341*, 249–259.
18. Schlegel H-G, Lafferty R, Krauss I. The isolation of mutants not accumulating poly-β-hydroxybutyric acid. *Arch. Mikrobiol.* **1970**, *71*, 283–294.
19. Zheng Y, Hong K, Wang B, Liu D, Chen T, Wang Z. Genetic diversity for accelerating microbial adaptive laboratory evolution. *ACS Synth. Biol.* **2021**, *10*, 1574–1586.
20. Badran AH, Liu DR. Development of potent in vivo mutagenesis plasmids with broad mutational spectra. *Nat. Commun.* **2015**, *6*, 1–10.
21. Wang X, Li Q, Sun C, Cai Z, Zheng X, Guo X, et al. GREACE-assisted adaptive laboratory evolution in endpoint

fermentation broth enhances lysine production by *Escherichia coli*. *Microb. Cell Factories* **2019**, *18*, 106.
22. Luan G, Cai Z, Li Y, Ma Y. Genome replication engineering assisted continuous evolution (GREACE) to improve microbial tolerance for biofuels production. *Biotechnol. Biofuels* **2013**, *6*, 1–11.
23. Wang J, Zhao D, Li J, Hu M, Xin X, Price MA, et al. Helicase-AID: A novel molecular device for base editing at random genomic loci. *Metab. Eng.* **2021**, *67*, 396–402.
24. Eom GE, Lee H, Kim S. Development of a genome-targeting mutator for the adaptive evolution of microbial cells. *Nucleic Acids Res.* **2022**, *50*, e38.
25. Asakura Y, Kojima H, Kobayashi I. Evolutionary genome engineering using a restriction–modification system. *Nucleic Acids Res.* **2011**, *39*, 9034–9046.
26. Nishida K, Arazoe T, Yachie N, Banno S, Kakimoto M, Tabata M, et al. Targeted nucleotide editing using hybrid prokaryotic and vertebrate adaptive immune systems. *Science* **2016**, *353*, aaf8729.
27. Komor AC, Kim YB, Packer MS, Zuris JA, Liu DR. Programmable editing of a target base in genomic DNA without double-stranded DNA cleavage. *Nature* **2016**, *533*, 420–424.
28. Xiong B, Li Z, Liu L, Zhao D, Zhang X, Bi C. Genome editing of *Ralstonia eutropha* using an electroporation-based CRISPR-Cas9 technique. *Biotechnol. Biofuels* **2018**, *11*, 1–9.
29. Tee KL, Grinham J, Othusitse AM, González-Villanueva M, Johnson AO, Wong TS. An efficient transformation method for the bioplastic-producing "Knallgas" bacterium *Ralstonia eutropha* H16. *Biotechnol. J.* **2017**, *12*, 1700081.
30. Wang Z, Pan H, Ni S, Li Z, Lian, J. Establishing CRISPRi for Programable Gene Repression and Genome Evolution in *Cupriavidus necator*. *ACS Synth. Biol.* **2024,** *13*, 851–861.
31. Lim HJ, Lee EH, Yoon Y, Chua B, Son A. Portable lysis apparatus for rapid single-step DNA extraction of *Bacillus subtilis*. *J. Appl. Microbiol.* **2016**, *120*, 379–387.
32. Li H, Durbin R. Fast and accurate short read alignment with Burrows-Wheeler transform. *Bioinformatics* **2009**, *25*, 1754–1760.
33. Li H, Handsaker B, Wysoker A, Fennell T, Ruan J, Homer N, et al. The Sequence Alignment/Map format and SAMtools. *Bioinformatics* **2009**, *25*, 2078–2079.
34. Wang K, Li M, Hakonarson H. ANNOVAR: Functional annotation of genetic variants from high-throughput sequencing data. *Nucleic Acids Res.* **2010**, *38*, e164.
35. Banno S, Nishida K, Arazoe T, Mitsunobu H, Kondo A. Deaminase-mediated multiplex genome editing in *Escherichia coli*. *Nat. Microbiol.* **2018**, *3*, 423–429.
36. Lada AG, Krick CF, Kozmin SG, Mayorov VI, Karpova TS, Rogozin IB, et al. Mutator effects and mutation signatures of editing deaminases produced in bacteria and yeast. *Biochemistry* **2011**, *76*, 131–146.
37. Grousseau E, Lu J, Gorret N, Guillouet SE, Sinskey AJ. Isopropanol production with engineered *Cupriavidus necator* as bioproduction platform. *Appl. Microbiol. Biotechnol.* **2014**, *98*, 4277–4290.
38. Lu J, Brigham CJ, Gai CS, Sinskey AJ. Studies on the production of branched-chain alcohols in engineered *Ralstonia eutropha*. *Appl. Microbiol. Biotechnol.* **2012**, *96*, 283–297.
39. Marc J, Grousseau E, Lombard E, Sinskey AJ, Gorret N, Guillouet SE. Over expression of GroESL in *Cupriavidus necator* for heterotrophic and autotrophic isopropanol production. *Metab. Eng.* **2017**, *42*, 74–84.
40. Frazao CJR, Wagner N, Rabe K, Walther, T. Construction of a synthetic metabolic pathway for biosynthesis of 2,4-dihydroxybutyric acid from ethylene glycol. *Nat. Commun.* **2023**, *14*, 1931.
41. Franden MA, Jayakody LN, Li WJ, Wagner NJ, Cleveland NS, Michener WE, et al. Engineering *Pseudomonas putida* KT2440 for efficient ethylene glycol utilization. *Metab. Eng.* **2018**, *48*, 197–207.
42. Muckschel B, Simon O, Klebensberger J, Graf N, Rosche B, Altenbuchner J, et al. Ethylene glycol metabolism by *Pseudomonas putida*. *Appl. Environ. Microbiol.* **2012**, *78*, 8531–8539.
43. Gaudelli NM, Komor AC, Rees HA, Packer MS, Badran AH, Bryson DI, et al. Programmable base editing of A*T to G*C in genomic DNA without DNA cleavage. *Nature* **2017**, *551*, 464–471.